Comprehensive Influence of Ultrasonic Vibration-Assisted Technology on Material Removal Mechanism under the Excitation of Regenerative Vibration in Precision Grinding Process

Yong Chen [1,*, a] Xun Chen [2, b] Zhongwei Hu[3,c] Nian Duan[1,d]

[1]College of Mechanical Engineering and Automation, Huaqiao University, Xiamen, 361021,

[2]General Engineering Research Institute, Liverpool John Moores University, Liverpool L3 3AF, U.K.

[3] Institute of Manufacturing Engineering, Huaqiao University, Xiamen, 361021, China

[a]42371502@qq.com(✉), [b]x.chen@ljmu.ac.uk, [c]huzhongwei@hqu.edu.cn, [d]dadamao1981@126.com

Abstract: Self-excited regenerative vibration, a well-known endogenous excitation mechanism, has a critical influence on material removal behavior and ground surface generation in a precision grinding process. During ultrasonic vibration-assisted grinding (UVAG), one-dimensional or two-dimensional ultrasonic vibration exerted to abrasive wheel or workpiece in axial and feed directions will influence material removing process significantly. Focusing on the study on the coupling relationship between ultrasonic vibration (as an external forced vibration) and regenerative vibration (as an internal vibration) excited by adjacent active abrasive grits, the improved theoretical models of cutting depth of abrasive grits and phase difference of grinding trajectory paths between adjacent active abrasive grits were presented in the paper with the consideration of the relationships between the ultrasonic vibration frequency, active abrasive grit number in contact zone and abrasive wheel speed. An optimization control strategy was further put forward by means of adjusting ultrasonic vibration frequency and the corresponding ratio to obtain proper phase difference of grinding trajectory paths of abrasive grits, which resulted to the improvement of cutting depth distribution and high surface finish of workpiece. The experiments of UVAG were conducted to verify the reliability of the influential mechanism and the validity of theorical model of cutting depth. Compared with the morphological characteristics of scratch section on the workpiece surface in axial cross-section before and after adjustment of ultrasonic vibration frequency, the results indicated that the numbers of active abrasive grits in contact zone increased with the increase of ultrasonic vibration frequency. When the vibration phase difference between grinding trajectory paths of adjacent abrasive grits was optimized to be an odd multiple of $\pi/2$ by stipulating proper ultrasonic vibration frequency, the vibratory amplitude of active abrasive

grits decreases. As a result, the cutting depth of abrasive grits and the distribution of workpiece surface waviness were comparatively uniform, and the average surface roughness measured in five groups of experiments decrease by up to 27% in comparing with those without UVAG. In contrast, when the vibration phase difference was an even multiple of $\pi/2$, the amplitude of workpiece surface waviness reached to its maximum due to the double excitation effects of regenerative vibration and ultrasonic vibration, the surface roughness worsened by 23%. The finding provides a clear guidance to the preparation of structured abrasive tools and matching strategy of process parameters in UVAG.

Key words: Ultrasonic vibration-assisted grinding (UVAG); Regenerative vibration mechanism; Cutting depth; Vibration phase difference; Surface topography

1 Introduction

Precision grinding is widely used to acquire high surface finish, where the material removal is performed by a large number of irregularly-positioned abrasive grits on grinding wheel surface under stable machining conditions [1, 2]. A stable grinding process is crucial to ensure machining accuracy and to prolong the life of machine tool and grinding tool. Two modes of vibration mechanisms widely studies by researchers in past decades [3]. The external forced vibration mainly derives from the transmission system of machine tool, including rotating motor spindle and moving workbench, or from the eccentric rotation behavior due to installation deviation between the grinding wheel and the wheel spindle, or partly from irregular wear of abrasive wheel. On the other hand, the internal self-excited regenerative vibration derives from the dynamic deviation of the cutting depth of each consequent active abrasive grits. The nonlinear coupling effect of both external vibration and internal vibration has a great influence on material removal in stable process, as shown in Figure 1, which makes it very difficult to quantitatively define and control the stability of precision grinding process and associated machining accuracy [4].

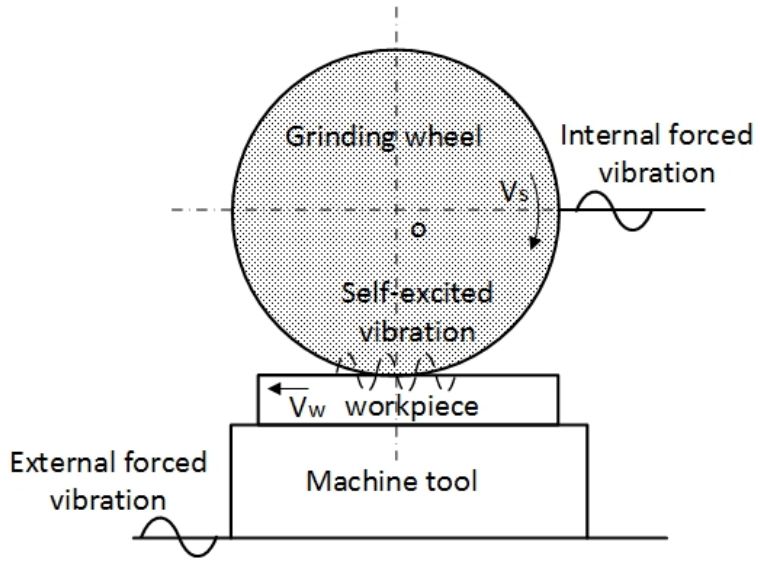

Fig. 1 Simplified kinematic model of forced vibration and self-excited regenerative vibration in grinding

Comparatively, the external forced vibration might be greatly reduced by optimizing the process conditions or cutting parameters, such as improving the overall rigidity of machine tool transmission system (including motor spindle and motion table, etc.) and the motion accuracy of the key transmission components, which ensures higher kinetic stability and machining accuracy during the grinding process [5]. Forced vibration is also obviously weakened by optimizing the online/offline dressing process condition of abrasive wheel prior to grinding [6], and adding online or offline dynamic balance auxiliary devices, which is helpful to avoid eccentric rotation behavior caused by installation error or wear deterioration of abrasive wheel [7]. However, an internal self-excited vibration is hardly “eliminated” completely. The regenerative vibration derives from intrinsic property of self-excited behavior due to the coupling relationship between the actual dynamic material removal and process variables (including cutting depth, grinding force, specific grinding energy, etc.) regardless the grinding of plastic or brittle materials. Based on material removal mechanism with varied cutting depth of the adjacent active abrasive grits at the same cutting-position of workpiece surface in continuous rotation cycles, a nonlinear time-delay vibration with certain amplitude and phase shift occurs in the contact zone between the abrasive grits and the workpiece, which further results in an instantaneous cutting depth deviation of adjacent active abrasive grits [8]. Rather than a constant, the varied instantaneous cutting depth affects overall process stability and machining accuracy [9].

Ultrasonic vibration-assisted grinding (UVAG) technology possesses many advantages, such as high processing efficiency [10] and quality surface and low process costs [11], for hard and brittle materials or difficult-to-machine materials [12]. Compared with the other traditional machining technologies, under conditions of exerting one-dimensional or two-dimensional ultrasonic vibrations derived from the ultrasonic transducer and horn that is assembled with abrasive wheel or workpiece, the material removal mechanism of UVAG technology is that the active abrasive grits distributed on surface of abrasive wheel conduct periodic material removal behaviors of "intermittent impact" and "discontinuous grinding" in corresponding axial and feed directions[13,14]. The "intermittent impact" promotes the short interactions between micro-cutting-edges of abrasive grits and workpiece [15] and produces the extremely high local stress in the workpiece leading to the generation [16,17] and propagation micro-crack and further local material fragmentation and removal [19,20]. According to the correlations between process parameters and ground surface quality in UVAG, Wang [12], Meng [13] and Zahedi [14] et al. studied the matching strategy on the UVAG process condition selections and proposed an optimization solution to improve machining quality of titanium alloy materials within a proper range of grinding speed. Aiming at the decrease of grinding force and the improvement of grinding wheel shape accuracy, Qiao et al. [15] studied the influence of UVAG on the truing/dressing of metal-resin-bonded diamond grinding wheel, and Ding[16-17], Huang[20] and Yang[21]et al. revealed that the increase of the ultrasonic amplitude could lead the decrease of truing/dressing force, the increase of material removal rate and a significant improvement of machining accuracy. Based on kinematic analysis of UVAG, Ding [17], Li [19] and Zhou [22] et al. presented the equations of matching relationship between ultrasonic vibration frequency, abrasive wheel diameter and some grinding parameters, and made a conclusion that ultrasonic vibration effect weakens with the increase of grinding speed, feed speed and total cutting depth with experimental verification.

Most of aforementioned researches mainly focus on the mechanism of intermittent impact, crack fragmentation and effective suppression technology of micro-crack propagation in machined hard and brittle materials during UVAG. Considering the double excitation of specified ultrasonic vibration and regenerative vibration, the material removal mechanism of abrasive grits that interacts with workpiece along a specific composite trajectory path corresponding to the UVAG

dynamics has not been studied and discussed yet. Accompanied with external ultrasonic vibration in the process, “negative” or “positive” influence of regenerative vibration on cutting depth of abrasive grit and material removal behavior is still not clear. Potential worsened situation should be properly controlled or avoided to satisfy the surface quality requirement.

In the paper, the influential mechanism of ultrasonic vibration on the instantaneous cutting depth of abrasive grits is presented. The phase characteristics of workpiece surface waviness derived from the regenerative vibration mechanism is analyzed in detail, and the correlative analytical model combining with ultrasonic vibration and regenerative vibration is developed. By comparing the scratch characteristics in axial cross-section of workpiece measured in precision grinding experiments under the conditions of with and without ultrasonic vibration at specified frequencies, the comprehensive influence of the simultaneous excitation of ultrasonic vibration and regenerative vibration on the surface topography of workpiece is depicted, and the strategy of ultrasonic vibration frequency optimization is proposed. Furthermore, the results of grinding experiments are presented to verify the reliability of the proposed strategy.

2 Material removal mechanism of the double excitation of regenerative vibration and ultrasonic vibration

2.1 Material removal behavior of the excitation of regenerative vibration

Based on regenerative vibration mechanism, the material removal model of an active abrasive grit is established at the time when the grit scratches through the wavy surface created by previous abrasive grits, as shown in Fig.2. Here, *X*-axis, *Y*-axis and *Z*-axis represent the normal direction, feed direction and axial direction of workpiece respectively. There are many abrasive grits in conical shapes (as an assumption) with small rounded apex positioned on the surface of grinding wheel laterally, as shown in Fig.2a (top right). The material removal mechanism is that a certain amount of material is removed away in pure shear mode by the continuously active abrasive grits irregularly or regularly distributed on surface of abrasive wheel during grinding process, which results to the formation of many staggered or overlapped scratch grooves on surface of workpiece, then surface topography of workpiece is generated along axial direction of abrasive wheel. A slim scratch with the certain length, width and depth is formed by a single grit, as shown in Fig.2a(right-bottom). Neglecting the influence of rubbing (sliding) and ploughing during the grinding process, the materials removal by a single abrasive grit *i* positioned on the surface of the

abrasive wheel can be illustrated in Fig.2a. When the abrasive wheel of radius R rotates around rotational center O at an angular velocity of ω (or at linear surface speed of abrasive wheel v_s) and the workpiece moves at feed speed v_w, the effective grinding radius of two adjacent active abrasive grits i and i-1 passing the position p in the contact zone can be presented as R_w(t) and R_w(t-T) respectively, where T is the time interval of these two grits pass the same cutting-position p. This results in an instantaneous radial cutting depth $h(\varphi_i)$ and generated workpiece surface topography with a specific waviness amplitude and a waviness phase, as shown in Fig.2b.

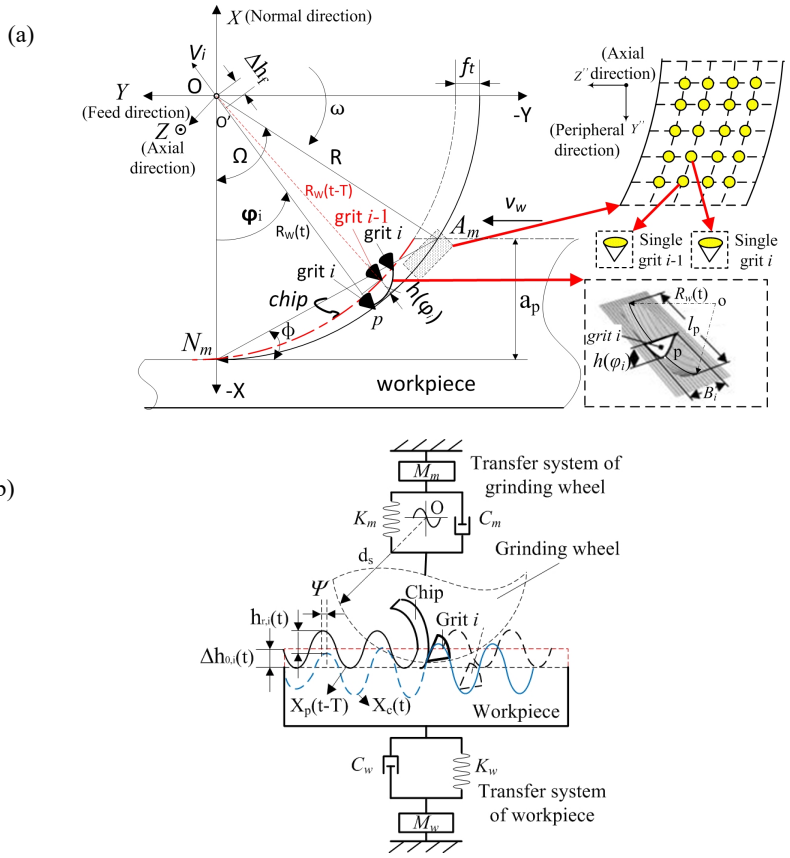

Fig.2 Material removal model based on regenerative vibration mechanism: **a** instantaneous cutting depth in down grinding, **b** analytical model of instantaneous cutting depth based on regenerative vibration mechanism

Grinding performance and machining accuracy are affected by many factors, such as the overall operation situation of machine tool, the grinding parameters and auxiliary lubrication cooling conditions etc [18][23][24]. Based on the chatter stability analysis of precision grinding in many researches, the conclusions demonstrate that the relative vibration (or even chatter) frequency between the abrasive wheel (i.e. abrasive grits) and the workpiece has a significant influence on the instantaneous radial cutting depth of abrasive grits [4][25]. As shown in Fig.2b, the vibration waviness numbered as $k+\sigma$ on the surface of workpiece was created by removing materials with a single active abrasive grit in the contact zone $\overline{A_mB_1}$, where k is a positive integer (k =1, 2, 3...), the physical meaning of variable σ is explained to be the phase difference

variable ψ derived from the vibration deviation of previous formed waviness (its amplitude is expressed by X_p) and the current waviness (its amplitude is expressed by X_c) divided by 2π, namely $\psi = 2\pi\sigma$, which can be taken as $0 \le \sigma < 1$. In Fig.2(b), the characteristic of phase difference ψ is closely related to the instantaneous cutting depth of continuously active abrasive grits.

2.2 Material removal behavior of the double excitation of regenerative vibration and ultrasonic vibration

On condition of ultrasonic vibration exerted in feed direction during grinding, the transient grinding point of the single abrasive grit *i* shown in Fig.2b is selected as a temporary coordinate origin o' and correspondingly, a local coordinate system in contact zone is established by taking radial and tangential directions around instantaneous grinding point as X'-axis and Y'-axis respectively, as shown in Figure 3.

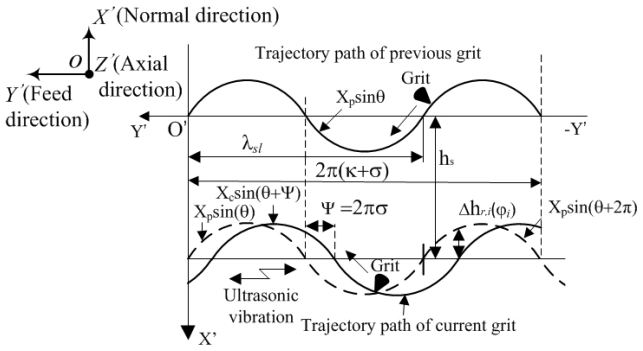

Fig. 3 Surface waviness generation of workpiece on condition of UVAG

Assuming the rotating speed of machine tool spindle or abrasive wheel is expressed by *n (*r/min*)*, the total number of active abrasive grits rotating with same radius in the axial cross-section (in *Z'* direction perpendicular to feed direction of workpiece) distributed evenly on the surface of abrasive wheel and continuously removing materials at the same surface position of workpiece is *m*, the number of active abrasive grits in the contact zone is m_g at the current time t when the position angle of grits is ϕ_i and the relative vibration frequency between the abrasive wheel and the workpiece is expressed by *f (*rad/s*)* (i.e. the ultrasonic vibration frequency exerted on the workpiece in the feed direction), *T* is the time interval between two adjacent abrasive grits removing material at the same surface position of the workpiece, then the relational expression of the vibration waviness on the workpiece surface in the contact zone created by the active abrasive grits after the grinding is calculated as:

$$f \cdot T = m_g(k+\sigma) = m_g(k+\frac{\psi}{2\pi}) \tag{1}$$

After transformed to: $$\frac{mn}{60} = \frac{1}{T} = \frac{f}{m_g(k+\sigma)} \tag{2}$$

According to Eq.2, it is shown that when the ratio of ultrasonic vibration frequency, wheel speed and the numbers of active abrasive grits in the contact zone during UVAG can be controlled to make the number of surface waviness in the contact zone as expressed on right side in Eq.1 as a positive integer, the wavy surfaces generated by two adjacent abrasive grits under ideal grinding situation will keep parallel to each other. This would lead to a constant cutting depth of abrasive grits, stable process and relatively smooth surface waviness. It is comparatively easy to adjust the ultrasonic vibration frequency and the wheel speed by means of changing stipulated process parameters, because the total number of active abrasive grits distributed on the surface of abrasive wheel remains relatively unchanged, when the diameter of wheel substrate base，the size of abrasive grits and the grit spacing distances are constant. In contrast, while the number of surface waviness in the contact zone is not integer, the surface waviness and the cutting depth of abrasive grits will be affected by overlapping excitation of regenerative vibration and ultrasonic vibration simultaneously, which result in the nonlinear deviation of the surface waviness created by the adjacent abrasive grits. The cutting depth will vary continuously in time domain during the grinding process and its value will reach to maximum, leading to the increase negative effect of "intermittent impact" and worsen surface quality.

As shown in Figure 3, the maximum amplitudes of surface waviness taken by two adjacent abrasive grits in the contact zone are X_c and X_p respectively, then the radial vibration displacements x_c and x_p of these two abrasive grits along the grinding trajectories path can be expressed as:

$$x_p(\theta) = X_p \sin \omega t = X_p \sin \theta \tag{3}$$

$$x_c(\theta+\psi) = X_c \sin(\omega t+\psi) = X_c \sin(\theta+\psi) \tag{4}$$

The instantaneous cutting depth deviation after continuous grinding can be calculated as:

$$\Delta h_{r,i}(\varphi_i) = x_p(\theta) - x_c(\theta+\psi) = X_p \sin(\theta) - X_c \sin(\theta+\psi) \tag{5}$$

In order to further solve the numbers of active abrasive grits in the contact zone expressed in Eq.2, the distribution of active grits uniformly positioned on the surface of the abrasive wheel is illustrated in Figure 4. Here, a temporary coordinate origin *O"* on the grinding wheel surface in contact zone is randomly selected and correspondingly, the local coordinate plane *O'-Y'-Z'* (along

the circumferential surface of abrasive wheel) in Figure 3 is rotated downwards and projected to the plane *O"-Y"-Z"* in axial and peripheral directions of the wheel in Fig.4a.

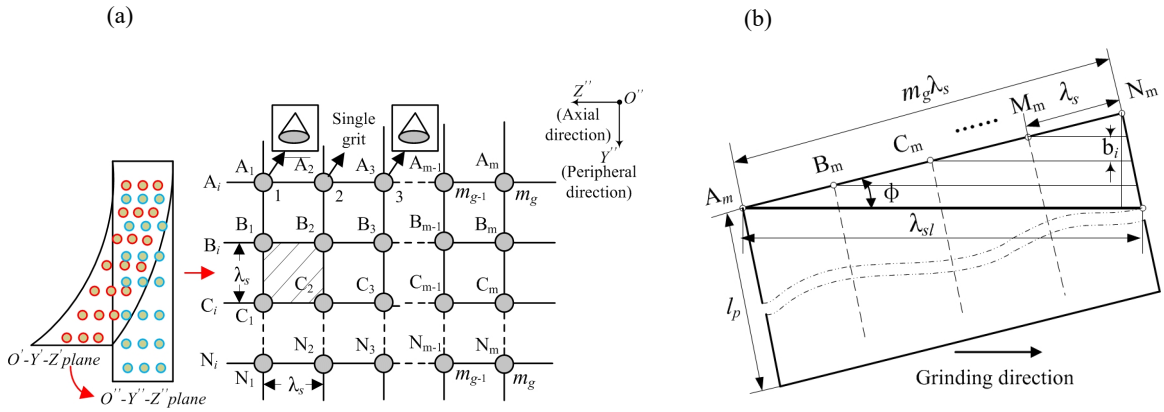

Fig. 4 Schematic diagram of active abrasive grits distribution on surface of abrasive wheel: **a** distribution of abrasive grits uniformly positioned on surface of abrasive wheel, **b** space distance of adjacent abrasive grits scratching through same position on surface of workpiece

It should be noted that in Fig.4a, λ_s is commonly defined as distribution spacing distance of abrasive grits uniformly positioned on surface of abrasive wheel in axial and peripheral directions. While in Fig.4b, λ_{sl} is described as cutting spacing distance of adjacent abrasive grits in tangential direction at same grinding point at the moment that workpiece material removed at feed speed. It means that the cutting edge of abrasive grit A_m will remove material at same surface position of workpiece, where the cutting edge of previous abrasive grit B_m just finished grinding along continuous grinding trajectory path at the interval time T. Therefore, different from λ_s in physical meaning, λ_{sl} is an important variable to determine the number of active abrasive grits in contact zone on surface of abrasive wheel by considering the trajectory path synthesis of grinding wheel and workpiece. Considering the irregular distribution of active abrasive grits, the mean value of $\overline{\lambda_s}$ is simplified and obtained by the designed measurement experiments of surface topography of abrasive wheel and adopted to calculate other corresponding machining variables. Accordingly, the material removal mechanism is analyzed more accurately by adopting the mean value of $\overline{\lambda_{sl}}$.

Assume the angle ϕ_i is corresponding to a wheel surface peripheral arc that has m_g active grits on it, the average cutting spacing distance of adjacent abrasive grits in the projection plane *O"-Y"-Z"* could be approximated as:

$$\overline{\lambda_{sl}} = \frac{m_g \cdot \overline{\lambda_s}}{\cos\phi_i} \tag{6}$$

Where: m_g is the number of active abrasive grits continuously arranged on the surface of the abrasive wheel in arc interaction zone. The number of m_g and the value of $\overline{\lambda_s}$ could be obtained by measuring the surface topography of abrasive wheel using Scanning Electron Microscope (SEM) imaging technology; $\phi_i=\omega t$ is the dynamic included position angle of grinding trajectory path of current active abrasive grits between peripheral direction and feed direction. Total position angle ϕ in contact zone shown in Fig.4b, as well as shown in Fig.2a, can be approximately calculated as [19]:

$$\sin\phi = \frac{a_p}{l_p} \tag{7}$$

Where, l_p is defined to be the arc length of contact zone, which can be calculated as:

$$l_p = \sqrt{a_p \cdot d_s} \tag{8}$$

Then:
$$\phi = \arcsin\sqrt{\frac{a_p}{d_s}} \tag{9}$$

Further the average scratch width between several grooves created by continuously active abrasive grits shown in Fig.4b is calculated as:

$$B_i = \frac{m_g \overline{\lambda_s}}{m_g - 1}\sin\phi_i \tag{10}$$

During the material removal process in one rotation cycle, the average chip volume is:

$$V_c = \overline{a_{g\max}} \cdot B_i \cdot l_p = \frac{a_p \cdot v_w}{\overline{\lambda_s} v_s} \tag{11}$$

Let chip shape ratio *r* to be:
$$r = B_i \Big/ \overline{a_{g\max}} \tag{12}$$

Combined with Eqs 8, 11 and 12, the theoretical value of average maximum undeformed chip thickness in contact zone during grinding is calculated as:

$$\overline{a_{g\max}} = \sqrt{\frac{v_w}{\overline{\lambda_s} \cdot r \cdot v_s} \cdot \sqrt{\frac{a_p}{d_s}}} \tag{13}$$

In one axial cross-section of abrasive wheel along peripheral direction, the total number of abrasive grits actively grinding is:

$$m = \frac{\pi \cdot d_s}{\overline{\lambda_{sl}}} \tag{14}$$

According to Eqs 2, 5, 6 and 14, it shows that under the condition of UVAG, the total number of active abrasive grits in the contact zone is closely related to the relative vibration frequency of the abrasive grit and the workpiece. The instantaneous cutting depth deviation of abrasive grits in radial direction has a close relation with the vibration amplitude and phase difference of the adjacent wavy surface taken by the consequent active abrasive grits. The phenomenon that the surface quality of machined workpiece worsens with the deterioration of dynamic wear of abrasive wheel could be explained as that the spacing distance of active abrasive grits will become larger due to worn grits fall off, leading to the decease of total number of abrasive grits participating in grinding. As a result, the instantaneous cutting depth deviation increases with the increase of phase difference of adjacent surface waviness on the excitation of ultrasonic vibration. Meanwhile, these changes will further strengthen "intermittent impact" effect during abrasive grits cutting in-out process, ultimately resulting in poor surface quality of machined workpiece. According to the analysis above, under the condition of UVAG as shown in Figure 3, the instantaneous cutting depth of abrasive grits at same grinding position will keep constant, grinding process tends to be relatively stable, and machining accuracy will be controlled in a relatively reasonable range by properly adjusting ultrasonic vibration frequency exerted on the workpiece in the feed direction, i.e. adjusting the phase difference of adjacent surface waviness of workpiece to be an odd integer multiple of $\pi/2$.

3 Experimental conditions and methods

Five groups of experiments were conducted to measure the mean value of surface roughness of ground workpiece and the correspondingly data analysis was carried out. The self-designed ultrasonic transducer and horn were assembled together to form an ultrasonic vibration device which resonance frequency was adjustable from 12~25 kHz, and the amplitude was adjustable from 0~12 μm. One rectangular support block was assembled between the machined workpiece and the feed table of machine tool by 2-4 binding bolts respectively. The experimental apparatus and measurement platform are illustrated in Figure 5 and experimental conditions are shown in Table.1. In the experiments of UVAG, adjustable ultrasonic vibration was exerted on workpiece in

feed direction, and a resin diamond abrasive wheel (diameter of wheel substrate base of 160 mm; abrasive grit size number of 60/85, average grit size of 0.25 mm, national standard ANSI-B74-16) was used to machine low-carbon steel workpiece that was fixed by two symmetrically arranged binding bolts on the support block with a single-stroke and dry grinding mode on MSG-250HMD grinding machine. Two piezoelectric accelerometers (Kistler 8764B) were respectively assembled on substrates of the support block and the abrasive wheel to collect vibration amplitude signals of workpiece and abrasive wheel in feed direction (motion direction of the worktable) and normal direction (perpendicular to motion direction of the worktable), meanwhile, to monitor the vibration amplitude of the ultrasonic horns in the range of designed limitation values. The sampling frequency of the accelerometers were set to 50kHz. Five different sampling zones in the sampling length of workpiece of 1-5 mm were selected to measure surface roughness by a Surface Roughness Measurement Instrument (MAHR MarSurf XR20), and the mean values of five groups of surface roughness characteristics of workpiece, including corresponding peak and valley amplitude of surface waviness in sampling zones, were obtained and evaluated offline machined surface quality improvement or deterioration. The characteristics of local axial cross-section profiles of three-dimensional surface topography, including cutting depth, groove width and length in contact zone at different intervals were measured by a Laser Confocal Detector (ZEISS LSM700). Furthermore, the material removal behavior conducted by the effective abrasive grits was discussed according to the characteristics varying tendency.

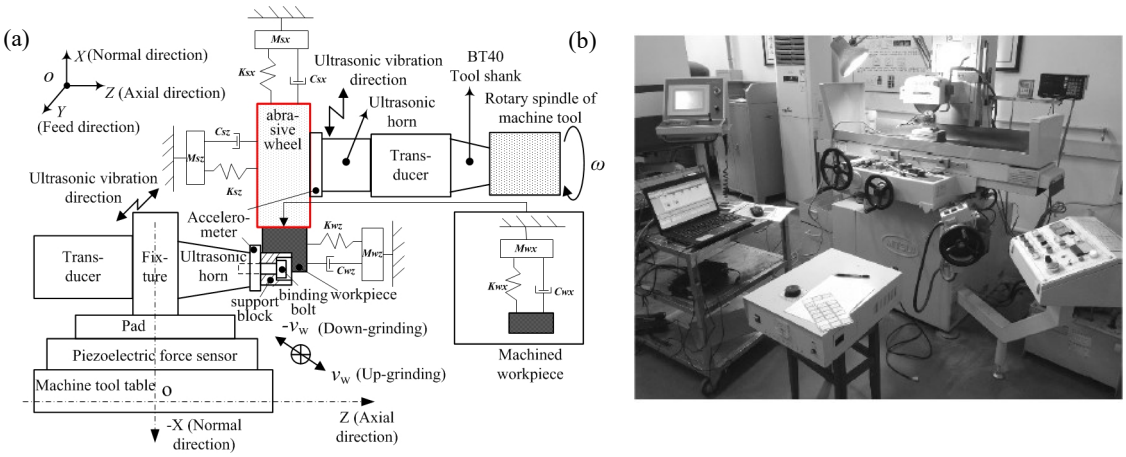

Fig. 5 Experimental apparatus of ultrasonic vibration-assisted grinding: **a** experimental principle, **b** measurement platform

Table 1 Experimental conditions of UVAG

Spindle speed ($r \cdot min^{-1}$)	Workpiece feed rate ($mm \cdot s^{-1}$)	Uniform distribution spacing of abrasive grits on surface of abrasive wheel (mm)	Average exposure height R_w of abrasive grits(mm)	Number of abrasive grits in per unit area (mm^2)
2880	150	0.45	0.125	16
Ultrasonic frequency f (kHz)	Horn amplitude (μm)	Grinding modes	Distribution spacing distance of abrasive grits λ_s (μm)	Total cutting depth a_p (μm)
12-25	0-12	single-stroke, dry grinding	0.45	5

4 Results and discussion

According to the conditions listed in Table1, including uniform distribution density of abrasive grits on surface of the resin diamond abrasive wheel and ultrasonic vibration frequency etc, by substituting the conditions into Eqs 6 and 14, total number of active abrasive grits in any axial cross-section of abrasive wheel is 1116 and the arc length of contact zone is 0.89 mm. The number of active abrasive grits in contact zone is about 2~4 varied with the increase of ultrasonic vibration frequency. While keeping the speed of machine tool spindle constant, the value of vibration phase difference of grinding trajectory paths is optimized to be an odd multiple of π/2 by changing the ratio between ultrasonic vibration frequency according to the changed numbers of active abrasive grits in contact zone and the speed of machine tool spindle. In this way, the vibration amplitude and cutting depth of abrasive grits are effectively controlled, so that the waviness distribution on surface of workpiece is uniform and higher machining accuracy is acquired. In contrast, when the vibration phase difference is adjusted to be an even multiple of π/2, the surface waviness amplitude of workpiece reaches to its maximum due to double excitation effects of regenerative vibration and ultrasonic vibration, machining quality is worsened accordingly.

As shown in Fig.6a, surface roughness of workpiece and local morphological characteristics of scratch section in axial cross-section are obtained by experimental measurement without UVAG. The mean value of surface roughness R_a of machined workpiece is 0.3509 μm. Four groups of experiments with UVAG are carried out by exerting various ultrasonic vibration frequencies on workpiece in feed direction, as shown in Fig.6b to Fig.6e separately. Especially, 3D topography and corresponding 2D profile of grooves in high frequency after UVAG are adopted to observe

scratches characteristics in Fig.6e.

By comparing scratches characteristics in Fig.6b to Fig.6e, the density of surface scratches in a cross-section in axial direction taken by active abrasive grits in the contact zone and amplitude of vibration cutting impact in UVAG tend to increase gradually with the increase of ultrasonic vibration frequency in sample area. Measured in UVAG experiments on various ultrasonic vibration frequency and other conditions unchanged, the average surface roughness R_a of machined workpiece and tendency of increasing or decreasing are listed in Table 2.

Table 2 Average R_a on various conditions

Conditions	Surface roughness R_a(um)	Tendency of increasing or decreasing of R_a comparing to the one without UVAG	Corresponding Fig.
Without UVAG	0.3509	--	Fig.6a
f = 12 kHz, m_g=2, Ψ=π/4	0.2538	↓27%	Fig.6b
f = 16 kHz, m_g =2, Ψ= π/2	0.2926	↓16%	Fig.6c
f = 21.4 kHz, m_g =3, Ψ= π	0.4334	↑23%	Fig.6d
f = 24.1 kHz, m_g =4, Ψ= 5π/2	0.328	↓7%	Fig.6e

In Fig.6b, the average surface roughness R_a of machined workpiece is 0.253 8 μm with low ultrasonic vibration frequency (f = 12 kHz, m_g=2, Ψ =π/4). In Fig.6c and Fig.6e, two optimized ultrasonic vibration frequency (f = 16 kHz and f = 24.1 kHz) were applied, the active abrasive grits in contact zone and phase difference between the consecutive surface waviness were m_g=2, Ψ = π/2 and m_g=4， Ψ = 5π/2, and the mean values of surface roughness R_a became 0.292 6 μm and 0.328 μm respectively. Compared with surface roughness value in experiment without UVAG, these values gradually decrease (i.e. the corresponding machining qualities improve) by nearly 27%，16%和 7% respectively. While the mean value of surface roughness R_a of machined workpiece under conditions of f = 21.4 kHz, m_g=3, Ψ = π is 0.433 4 μm shown in Fig.6d. The (a) ： is about 1.5 time larger than that with f = 16 kHz, m_g=2, Ψ = π/2 (i.e. Ψ is an odd multiple of π/2) and the accuracy decreases (i.e. the corresponding machining quality becomes worse) by nearly 23% by comparison with that measured without UVAG. Based on analysis of mentioned above, ground surface quality of workpiece is not improved, while there is a downward trend by applying UVAG technology in precision grinding if proper matching strategy of process parameters, including optimization of the ratio between ultrasonic vibration frequency, speed of machine tool spindle and active abrasive grits in contact zone is not reasonably optimized.

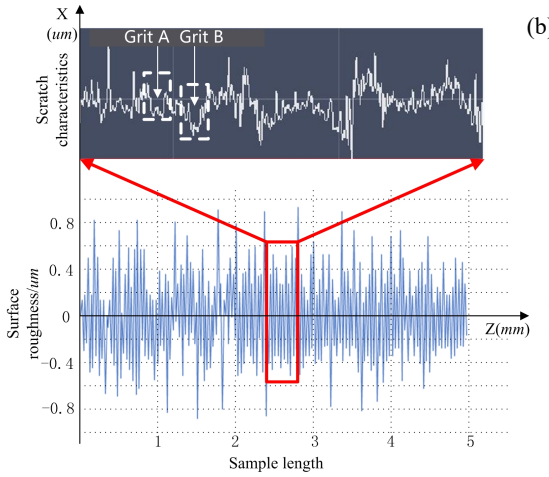
X
(um)
Grit A Grit B
Scratch characteristics
0.8
0.4
0
−0.4
−0.8
Surface roughness/um
Z(mm)
1
2
3
4
5
Sample length

(b)

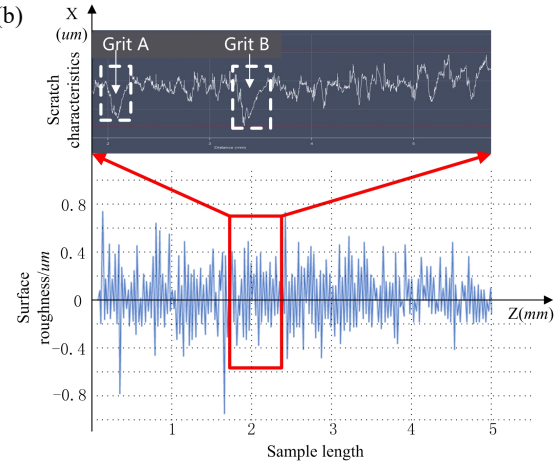
X
(um)
Grit A
Grit B
Scratch characteristics
0.8
0.4
0
−0.4
−0.8
Surface roughness/um
Z(mm)
1
2
3
4
5
Sample length

(c)

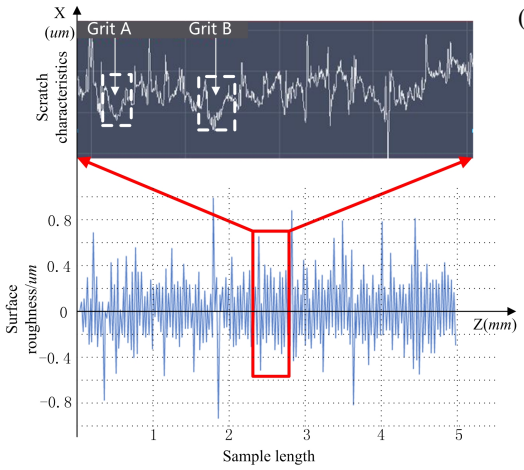
X
(um)
Grit A
Grit B
Scratch characteristics
0.8
0.4
0
−0.4
−0.8
Surface roughness/um
Z(mm)
1
2
3
4
5
Sample length

(d)

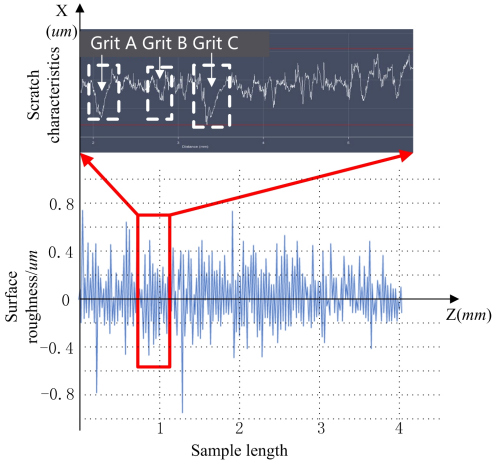
X
(um)
Grit A Grit B Grit C
Scratch characteristics
0.8
0.4
0
−0.4
−0.8
Surface roughness/um
Z(mm)
1
2
3
4
Sample length

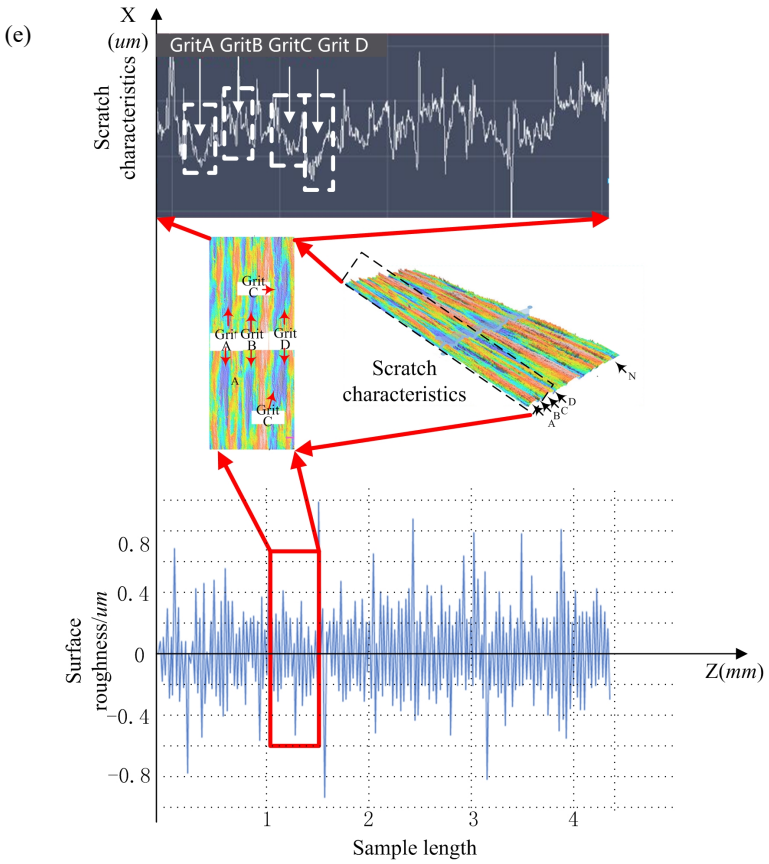

Fig.6 Surface roughness and morphology characteristics of machined workpieces without and with UVAG: **a** without ultrasonic vibration, **b** f = 12 kHz, m_g=2, **c** f = 16 kHz, m_g=2, **d** f = 21.4 kHz, m_g=3, and **e** f = 24.1 kHz, m_g=4

Furthermore, Fig.6b and c show that the process in UVAG is more stable and the scratches depths are smaller compared with the results without applying UVAG. With the increase of ultrasonic vibration frequency, as shown in Fig.6c, the amplitude of local vibration caused by intermittent impact of abrasive grits in-out cutting becomes larger obviously. Most of morphology feature amplitudes distributed stably in the range of [-0.38 ~ 0.52] μm after calculating average values of valleys and peaks of the scratch grooves. Looking at two large scratches cut by abrasive grits (A and B) with large protrusion heights, it is observed that cutting depths and scratches width of the grits are evenly and smoothly distributed on surface of workpiece, and most of morphology feature amplitudes distributed stably in the range of [-0.32 ~ 0.23] μm in axial cross-section.

Similar data analysis is conducted in Fig.6d. The results indicate that even though the surface quality of machined workpiece becomes slightly better by nearly 7% than that measured without UVAG, UVAG process is well uesed in actual application due to higher machining efficiency and more active abrasive grits(3 grits) in contact zone. Although there are more abrasive grits(4 grits A to D in same sample length) and regularly intermitten scratch grooves observed on 3D ground surface in Fig.6e due to higher ultrasonic vibration frequency, morphology characteristics of

scratch section becomes more complex with obvious oscillation and instantaneous cutting depth of abrasivegrits is larger on double excitation of regenerative vibration and ultrasonic vibration, as shown in Fig.6e. Most of the morphology amplitudes of surface section is distributed in larger range of [-0.42 ~ 0.58] μm, which implies unsatisfactory surface quality of workpiece is acquired.

5 Verification of theorical models of instantaneous cutting depth

According to the analytical models shown in Eq.5 and Eq.11, under same experimental conditions as those in Fig.6c and same sample area of 0.5 mm, the motion trajectory of active working grits scratching through the contact zone are calculated. The experimental results and the virtual 3D surface topography of workpiece are observed in Fig.7a, b separately.

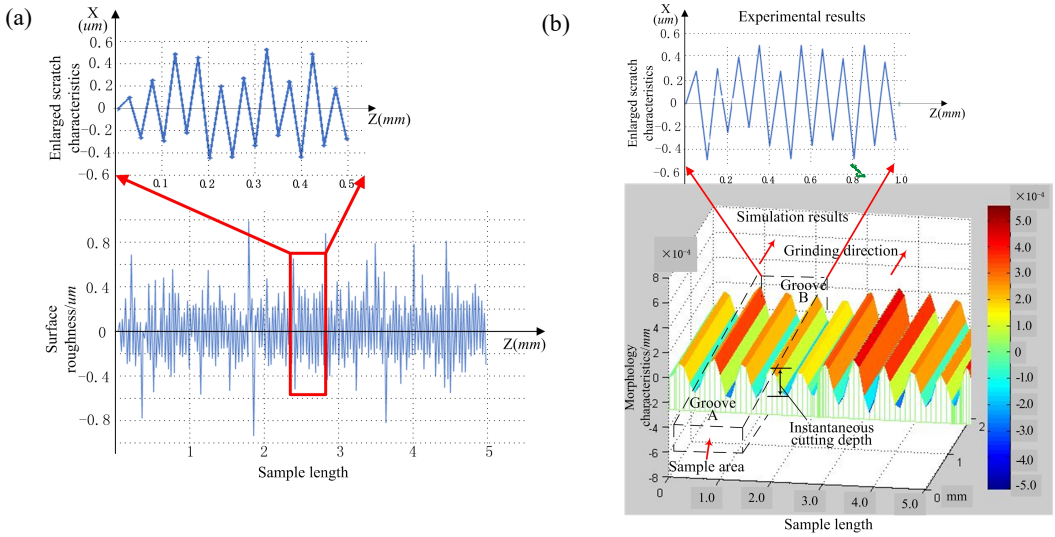

Fig.7 Surface topography of machined workpiece at ultrasonic vibration frequency f = 16 kHz: **a** experimental results of surface topography, **b** simulation results of surface topography

Compared with experimental results of morphology characteristics in range of [-0.38 ~ 0.52] μm with mean value of 0.29 μm shown in Fig.7a during stable process, most of theorical results of surface characteristics between the maximum peak and the deepest valley are concentrated in the range of [-0.41 ~ 0.43] μm with mean value of 0.26 μm, as shown in Fig.7b. The prediction error of theorical model of cutting depth is about 10%. Similarly, when the experimental parameters same as those in Fig.6e are adopted to calculate theorical cutting depth, most of theorical surface characteristics between the peak and the valley are concentrated in the range of [-0.43~ 0.45] μm with mean value of 0.32 um, while most of experimental results of the morphology characteristics distributed in larger range of [-0.42 ~ 0.58] μm, which implies unstable process. The prediction error of theorical model of cutting depth reaches to 22.5%. It implies that it is more difficult to predict cutting depth in high accuracy with standard theorical models with the increase of

“negative” influence of the “intermittent impact” (i.e. external forced vibration) during UVAG.

6 Conclusions

The influential mechanism of ultrasonic vibration on regenerative vibration and material removal behavior is crucial to monitor process stability and acquire satisfactory surface finish of workpiece in UVAG. In the paper, an improved model of instantaneous cutting depth of adjacent active abrasive grits during UVAG is developed and comprehensive influence of ultrasonic vibration and regenerative vibration on material removal mechanism is studied. The corresponding matching strategy of process parameters is proposed to acquire high-precision ground surface by means of optimizing the ratio of related grinding parameters and the phase difference of vibration waviness on surface of workpiece. The conclusions demonstrate:

1) The instantaneous cutting depth of active abrasive grits is greatly affected by double excitation of ultrasonic vibration and regenerative vibration during UVAG. The surface quality of machined workpiece could be reduced, rather than being improved as proper matching strategy of process parameters, including optimization of the ratio between ultrasonic vibration frequency, speed of machine tool spindle and active abrasive grits in contact zone is not reasonably adopted in UVAG.

2) In UVAG, high machining accuracy is acquired when the value of vibration phase difference of grinding trajectory paths is equal to be an odd multiple of $\pi/2$ by optimizing the ratio between ultrasonic vibration frequency and the correspondingly changed number of active abrasive grits in contact zone and speed of machine tool spindle. The mean values of surface roughness measured in experiments with the optimized ratio decrease (i.e. the corresponding machining qualities improve) by up to 27% by comparing with those without UVAG. The cutting depths and width of the scratches are evenly and smoothly distributed on surface of workpiece.

3) Morphology characteristics of scratche section becomes more complex and its value reaches to maximum with unstable oscillation on double excitation of regenerative vibration and ultrasonic vibration when the value of vibration phase difference of grinding trajectory paths is equal to be an even multiple of $\pi/2$. The mean value of surface roughness on double excitation is about 1.5 time larger than those with the optimized ratio or phase difference of consecutive vibration waviness and decreases (i.e. the corresponding machining quality worsen) by nearly 23% by comparison with that in experiment without UVAG, which implies unsatisfactory surface quality of workpiece is acquired.

Declarations

Funding

This work was supported by the National Natural Science Foundation of China (Grant number [52175404]). Author Zhongwei Hu has received research support from the National Natural Science Foundation of China.

Competing Interests

The authors have no relevant financial or non-financial interests to disclose.

Author Contributions

All authors contributed to the study conception and design. The first draft of the manuscript was written by Yong Chen. The methodology and conceptualization of the manuscript were presented by Yong Chen. The supervision and review of the manuscript were performed by Xun Chen. Material preparation, data collection and analysis were performed by Zhongwei Hu and Nian Duan. All authors commented on previous versions of the manuscript. All authors read and approved the final manuscript.

Reference

1. Chen X, Rowe WB(1996) Analysis and simulation of the grinding process. Part III: Mechanics of grinding. Int J Mach Tools Manuf 36(8):883-896. https://doi.org/10.1016/0890-6955(96)00116-2

2. Aurich JC, Kirsh B (2012) Kinematic simulation of high-performance grinding for analysis of chip parameters of single grits. CIRP J Manuf Sci Technol 5(3):164-174. https://doi.org/ 10.1016/j.cirpj.2012.07.004

3. Chen Y, Chen X, Xu XP, Yu G(2018). Quantitative impacts of regenerative vibration and abrasive wheel eccentricity on surface grinding dynamic performance. Int J Adv Manuf Technol 96: 2271-2283. https://doi.org/10.1007/s00170-018-1778-3

4. Huseyin C, Erdem O, Neil DS(2021) Can mode coupling chatter happen in milling? Int J Mach Tools Manuf 165(1):1-13. https://doi.org/10.1016/j.ijmachtools.2021.103738

5. Hu ZW, Chen Y, Lai ZY, Yu YQ, Xu XP, Peng Q, Zhang L(2022) Coupling of double grains enforces the grinding process in vibration-assisted scratch: Insights from molecular dynamics. J Mater Processing Tech 304: 1-14. https://doi.org/10.1016/j.jmatprotec.2022.117551

6. Chen Y, Hu ZW, Jin JF, Li L, Yu YQ, Peng Q, Xu XP(2021) Molecular dynamics simulations of scratching characteristics in vibration-assisted nano-scratch of single-crystal silicon. Appl Surf Sci 551(3): 1-11. https://doi.org/10.1016/j.apsusc.2021.149451

7. Kumar J(2013) Ultrasonic machining-a comprehensive review. Mach Sci Technol 17(3): 325-379. https://doi.org/ 10.1080/10910344.2013.806093

8. Wang B, Liu ZQ, Cai YK, Luo XC, Ma HF, Song QH, Xiong ZH(2021) Advancements in material removal mechanism and surface integrity of high speed metal cutting: A review. Int J Mach Tools Manuf 165:1-13. https://doi.org/10.1016/j.ijmachtools.2021.103744

9. Chen Y, Chen X, Xu XP, Yu G(2018) Effect of energy consumption in the contact on machining condition optimization in precision surface grinding. J Mech Eng 64:233-244. https://doi.org/

10.5545/sv-jme.2017.4995
10. Sharma A, Kalsia M, Uppal AS, Babbar A, Dhawan V(2022) Machining of hard and brittle materials: a comprehensive review. Mater Today Proc 50(5):1048-1052. https://doi.org/10.1016/j.matpr.2021.07.452
11. Tian ZG, Chen X, Xu XP (2020) Molecular dynamics simulation of the material removal in the scratching of 4H-SiC and 6H-SiC substrate. Int J Extrem Manuf 4(2): 86-100. https://doi.org/10.1088/2631-7990/abc26c
12. Wang Y, Lin B, Wang SL(2014) Study on the system matching of ultrasonic assisted grinding of hard and brittle materials processing. Int J of Mach Tools Manuf 77:66-73. http://dx.doi.org/10.1016/j.ijmachtools.2013.11.003
13. Meng B, Yuan D, Xu S(2019) Coupling effect on the removal mechanism and surface/subsurface characteristics of SiC during grinding process at the nanoscale. Ceram Int 45: 2483-2491. https://doi.org/10.1016/j.ceramint.2018.10.175
14. Zahedi A, Tawakoli T, Akbari J(2015) Energy aspects and workpiece surface characteristics in ultrasonic-assisted cylindrical grinding of alumina-zirconia ceramics. Int J Mach Tools Manuf 90:16-28. http://dx.doi.org/10.1016/j.ijmachtools.2014.12.002
15. Qiao JP, Wu HQ, Sun LH, Feng M, Zeng J, Wu YB(2022) Experimental investigation on ultrasonic-assisted truing/dressing of diamond abrasive wheel with cup-shaped GC wheel. Int J Adv Manuf Technol 121: 1717-1730. https://doi.org/10.1007/s00170-022-09397-5
16. Ding K, Fu YC, Su HH(2017) Experimental studies on matching performance of grinding and vibration parameters in ultrasonic assisted grinding of SiC ceramics. Int J Adv Manuf Technol 88: 2527-2535. https://doi.org/10.1007/s00170-016-8977-6
17. Ding WF, Cao Y, Zhao B, Xu JH(2022) Research status and future prospects of ultrasonic vibration-assisted grinding technology and equipment. J Mech Eng 58:244-269. https://doi.org/10.3901/JME.2022.09.244
18. Malkin S, Cai G(2008) Grinding technology-Theory and applications of machining with abrasive. Industrial Press, New York.
19. Li C, Zhang FH, Meng BB, Liu LF, Rao XS(2017) Material removal mechanism and grinding force modeling of ultrasonic vibration assisted grinding for SiC ceramics. Ceram Int 43:2981-2993. https://doi.org/10.1016/j.ceramint.2016.11.066
20. Huang WH, Yan JW(2023) Towards understanding the mechanism of vibration-assisted cutting of monocrystalline silicon by cyclic nanoindentation. J Mater Proc Tech 311: 1-18. https://doi.org/10.1016/j.jmatprotec.2022.117797
21. Yang X, Gao S(2022) Analysis of the crack propagation mechanism of multiple scratched glass-ceramics by an interference stress field prediction model and experiment. Ceram Int. 48: 2449–2458. https://doi.org/10.1016/j.ceramint.2021.10.026
22. Zhou W, Tang J, Chen H, Shao W(2019b) A comprehensive investigation of surface generation and material removal characteristics in ultrasonic vibration assisted grinding. Int J Mech Sci 156: 14–30. https://doi.org/10.1016/j.ijmecsci.2019.03.026
23. Wu YQ, Mu DK, Huang, H(2020) Deformation and removal of semiconductor and laser single crystals at extremely small scales. Int J Extrem Manuf 2(1): 109-134. https://doi.org/ 10.1088/2631-7990/ab7a2a
24. Huang H., Li XL, Mu DK, Lawn BR(2021) Science and art of ductile grinding of brittle solids. Int J Mach Tools Manuf 161: 1-15. https://doi.org/10.1016/j.ijmachtools.2020.103675

25. Agarwal S, Rao PV(2012) Predictive modeling of undeformed chip thickness in ceramic grinding. Int J Mach Tools Manuf 56: 59-68. https://doi.org/10.1016/j.ijmachtools.2012.01.003